Desalination and Water Treatment
www.deswater.com
doi: 10.1080/19443994.2013.844084

53 (2015) 603–609
January

Taylor & Francis
Taylor & Francis Group

Pretreatment of saline wastewater with Fe–C alloy filler

Guizhong Zhou*, Xuan Wang, Jianting Liu, Zhaofeng Wang, Shaoxiang Li

College of Environment and Safety Engineering, Qingdao University of Science and Technology, Qingdao 266042, P.R. China
Tel. +86 532 84022739; Fax: +86 532 84022617; email: zhougz@126.com

Received 2 May 2013; Accepted 5 September 2013

ABSTRACT

Fe–C alloy filler was prepared using iron powder and activated carbon. And it was proved to be efficient in getting rid of chloride from water, especially saline wastewater. Generally, biochemical treatment efficiency will be low if the concentration of chloride ion (Cl^-) in water reaches 10,000 mg/L. Once the Cl^- content exceeds 20,000 mg/L, most microbes will lose activity because of the high osmotic pressure. Besides, it will not only affect the microbes' survival but also be toxic to the microorganisms. This paper studied chloride removal efficiency with iron-carbon alloy. Factors affecting the removal efficiency and the possible removal mechanism were also investigated. Treatment effect for actual salinity wastewater with the filler was reported. The results showed that the new filler could effectively remove chloride ions and chemical oxygen demand (COD). COD_{Cr} removal rate of the chosen practical wastewater samples was higher than 55%, and the Cl^- removal rates were 27%, 30% and 25%, respectively. The oxygen consumption curves of the wastewater that were obtained from chemical industries showed that the biodegradability of wastewater could be greatly improved due to removal of Cl^- using the new filler.

Keywords: Fe–C alloy filler; Wastewater desalination; Cl^- removal mechanism; Oxygen consumption curve; Biodegradability

1. Introduction

Hypochlorous acid, hydrochloric acid and chlorinated compounds are widely used in industries like printing and dyeing, papermaking, chemical and pesticide, which can produce a lot of Cl^--containing wastewater. Wastewater with high concentrations of organic compounds and chloride is difficult to be biodegraded; so desalination is needed.

Traditional desalination technology is not merely expensive, energy-intensive, and time-consuming, but also ineffective [1]. Methods such as dilution after biochemical, multi-effect evaporation and membrane separation have been used for salinity wastewater treatment [2–4], but the problem of high cost and low treatment efficiency still remains unsolved.

Based on such a number of primary batteries formed within the filler, Fe–C micro electrolysis is widely used for the pretreatment of non-biodegradable wastewater [5,6]. However, this technique has not been widely used for chloride removal, and most of the micro-electrolysis fillers used in studies were a simple mixture of iron grain and carbon particles,

---

*Corresponding author.

1944-3994/1944-3986

which are prone to hardening and passivation in the actual wastewater treatment.

In this paper, a kind of iron-carbon alloy-based filler was developed. The large specific surface area and high reaction activity of the alloy showed surprising performance. Powders of iron and activated carbon were pressed and roasted to produce the alloy according to a certain proportion. The new filler had several advantages. First, iron and carbon were not easy to separate. Second, the integration of iron and carbon could improve electron transport performance and reaction efficiency. Finally, the structure could avoid passivation of iron and carbon.

Factors that influence Cl^- removal efficiency, including initial pH, residence time, concentration of chloride ions and organic matter content were studied. The Cl^- content in the respective reaction parts were confirmed through intermittent and continuous experiments. The removal pathway and removal mechanism of Cl^- were studied. The new filler was also used for treating actual salinity wastewater (such as modified starch wastewater, pharmaceutical wastewater, cellulose ether wastewater) to investigate the treatment effect.

2. Experimental

2.1. Materials and methods

2.1.1. Experimental raw water

Both simulated and actual wastewaters were used in this study. The simulated wastewater was prepared with NaCl solution. The actual wastewater samples that contain high concentrations of Cl^- were obtained from chemical industries. The characteristics of the actual wastewater are shown in Table 1.

Table 1
Characteristics of the actual wastewater

Items	Modified starch wastewater	Pharmaceutical wastewater	Cellulose ether wastewater
pH	4.57	6.74	5.65
NH_3-N	63.09 mg/L	12.32 mg/L	9.16 mg/L
Cl^-	20,880 mg/L	21,500 mg/L	15,360 mg/L
COD_{Cr}	23,520 mg/L	5,890 mg/L	12,400 mg/L

2.1.2. Filler of iron and carbon alloy

Iron fillings (mesh size less than 60) and activated carbon powder (mesh size less than 100) were used as raw materials. The iron fillings were activated by washing with 5% hydrochloric acid. The raw materials were first pressed under a pressure of 200 KN according to the proportion of iron fillings. The molding materials were then calcined under in the temperature range of 1,050–1,200°C for 90–100 min [7,8] in nitrogen atmosphere. Fig. 1 shows the appearance of the molding filler.

The micro-electrolysis reactors (MER) made of transparent polyvinyl chloride are shown in Fig. 2. The effective volume of the MER was 2 L. Wastewater was poured into the reactor at a constant flow rate using a flow pump. Aeration devices were at the bottom of the Fe–C MER and the fillers were in the middle. And the mode of aeration devices was continuous aeration. The wastewater entered into the tower from the bottom and came out from the top. After a period of reaction, the effluent was adjusted to alkaline environment (pH 9 or so) with NaOH and HCl, then about 0.3 mL PAC (2% w/v) and 0.1 mL PAM (2‰ w/v) were added per liter of wastewater for sedimentation [9]. Finally, the supernatant fluid was taken for testing. Batch experiment means that all the raw water was directly poured into the reactor at once, and then the effluence was taken out for

Fig. 1. Appearance of filler.

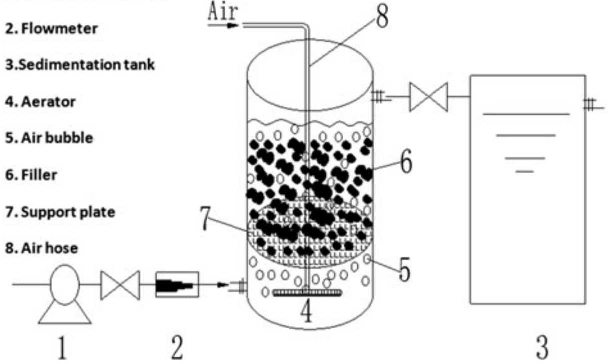

Fig. 2. Schematic diagram of experimental set-up.

flocculation precipitation after a certain reaction time. On the contrary, raw water was poured into the reactor continuously in the dynamic experiment, and the residence time was controlled by the flowrate [10].

2.2. Experimental procedures

Effects of reaction time, initial pH, Cl^- concentration and COD_{Cr} content on Cl^- removal efficiency were investigated through single factor experiment using simulated wastewater.

Under optimized conditions, take the NaCl solution containing 5×10^4 mg/L Cl^- as the raw wastewater. In order to determine the main removal pathway of Cl^-, batch experiments were carried out to detect the Cl^- concentration of effluent water, flocculation sedimentation and the filler. Meanwhile, the releasing gas was absorbed by 4% sodium hydroxide. Then, through continuous experiments, fillers before and after the reaction were tested to study the changes in surface structure and composition of the matter.

For practical salinity wastewater, the optimal reaction conditions were determined through single factor and orthogonal experiments. COD_{Cr} and Cl^- removal rate and the biodegradability of wastewater after reactions were measured, respectively, under the optimal reaction conditions [11–13].

2.3. Analytical methods

For water quality, COD_{Cr}, pH and Cl^- were measured by the China national standard methods or the recommended standards of the environment protection sector [14]. Chemical oxygen demand analyzer (HACH DR 200, DR 2700) was used for the detection of COD_{Cr}. Biodegradability of the wastewater was measured with a fluorescent dissolved oxygen meter (HACH, HQ30D).

For filler performance detection, the iron-carbon alloy before and after the reaction was crushed into powders (without grains) and particles (diameter of 2 mm), respectively, and was observed with a scanning electron microscope (SEM) (JSM-6700F, JEOL) and X-ray scanning (INCA energy, oxford instruments). The specific surface area of the filler was measured by fully automatic surface area and pore size analyzer (V-Sorb 2800P, Beijing Jin Ai Pu Science and Technology Company Limited). Through the analysis of the results, the surface morphology and changes in the phase were identified.

3. Results and discussion

3.1. Removal of Cl^- by the iron carbon alloy

3.1.1. Concentration

Fig. 3(A) shows the effect of the initial Cl^- concentration on the removal rate at room temperature. To discuss the treatment effects of different initial Cl^- concentrations, Cl^- concentration of raw water ranges from 5×10^3 to 5×10^4 mg/L with the initial pH fixed as 2 for a reaction time of 60 min. Fig. 3(A) shows that the removal rate of Cl^- could reach about 25% among the studied scope with minor fluctuations.

3.1.2. pH

Fig. 3(B) shows the effect of the initial pH on the removal rate at room temperature. Sodium hydroxide solution (30% w/v) and sulphuric acid solution (30%

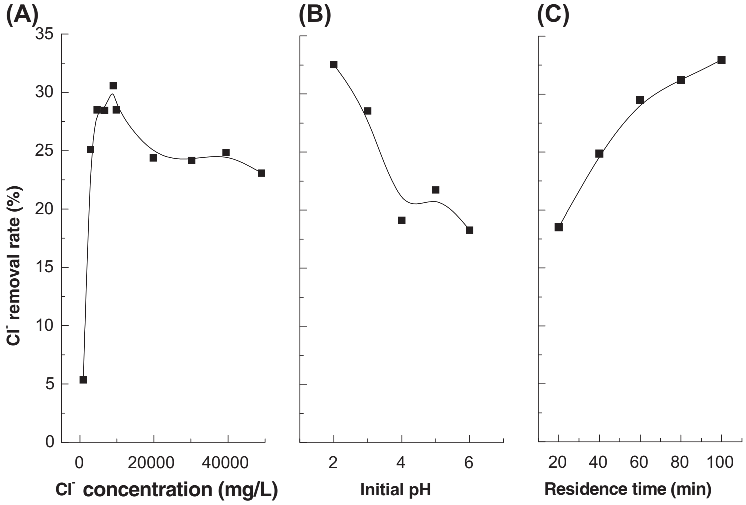

Fig. 3. Effect of the initial Cl^- concentration, initial pH and residence time on the removal rate.

v/v) were used to change the pH. The initial pH of raw water was adjusted to 2, 3, 4, 5 and 6, respectively, with the initial Cl$^-$ concentration fixed as 20,000 mg/L for the reaction time of 60 min. Fig. 3(B) shows that the Cl$^-$ removal rate can reach as high as 32.5% while the pH is 2. It tells that the pH has a greater impact on the Cl$^-$ removal rate for the new filler.

3.1.3. Residence time

Fig. 3(C) shows the effect of residence time on the removal rate at room temperature. To discuss the factor of residence time, the residence time of the reaction was set to 30, 60, 90, 120, 150 and 180 min with the initial pH fixed as 4 and Cl$^-$ concentration fixed as 20,000 mg/L. At first the removal rate of Cl$^-$ increased significantly as the residence time was prolonged, after 60 min, there is only a less variation, hence consider a retention time 60 min as the best condition for this research.

3.2. The Cl$^-$ removal mechanism of the filler

Sodium chloride solution with a Cl$^-$ concentration of 20,000 mg/L was prepared as the raw water. The removal rate of Cl$^-$ could reach approximately 25% through repeated experiments. Among the 25%, only a small part was oxidized to Cl_2, even a smaller part was removed through flocculation and most of the Cl$^-$ was absorbed by micro electrolysis fillers (Fig. 4). Adsorption of Cl$^-$ happened mainly through two mechanisms: (1) activated carbon within the filler could absorb some Cl$^-$; (2) micro-electric field caused by the micro-electrolysis reaction in filler cavities gave the filler surprising electrosoption capacity of Cl$^-$. Such a removal rate was mainly attributed to the second mechanism. For electric-absorption, Cl$^-$ was also driven by electric field force, and it is stronger and more selective than free diffusion of physical adsorption.

For the experiments, Cl$^-$ was removed mainly through adsorption by the filler. Although activated carbon in the filler had physical adsorption ability, Cl$^-$ was absorbed mainly through electric-absorption caused by the primary cell reaction of the Fe–C alloy. Cavities inside the filler acted as the primary cell and provided micro-electric field. Cl$^-$ in the midst of the cavities was electrically driven onto the surface of electrodes [15–17].

To study the adsorption capacity of the filler, the Cl$^-$ concentration of the influent was detected continuously with the reaction conditions fixed. As shown in Fig. 5, at the beginning of the reaction, the Cl$^-$ removal rate was high, and then it reduced gradually with lapse of the reaction time. After 90 min, the Cl$^-$ removal rate dropped to 2.5%, illustrating that the filler was close to adsorption saturation [18].

The composition and surface structure of the filler were analyzed. Fig. 6 shows the results of the XRD. Through comparison, it was clear that the filler after reaction had obvious diffraction peaks at the 2-θ angle of 31 degrees which corresponds to the phase of NaCl [19,20], confirming that the filler had strong adsorption to Cl$^-$.

The SEM photograph showed that the filler was a porous material with rough surface ((A) and (B) of Fig. 7). The specific surface area was 1.1 m^2/g measured through the method of nitrogen adsorption. Also, the porous structure can improve electron transfer efficiency and increase the electron pairs of

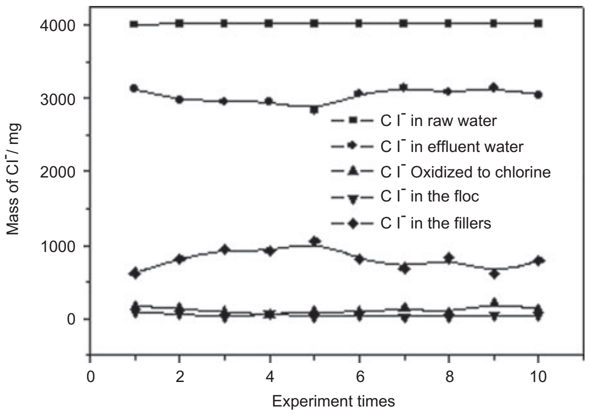

Fig. 4. Cl$^-$ content analysis of multiple batch experiment.

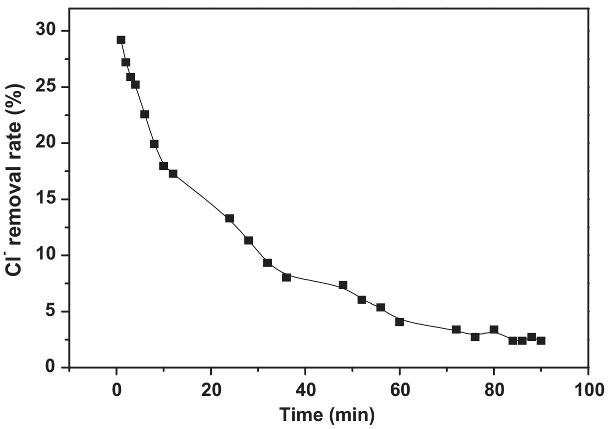

Fig. 5. Cl$^-$ removal rate at different running times.

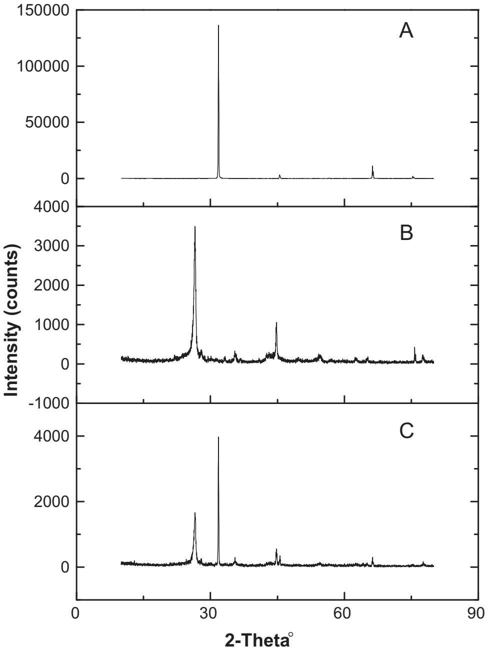

Fig. 6. XRD result of pure NaCl, the filler before and after reaction.

the micro-electrolysis process [7,8]. The large specific surface area and the number of cavities make electric adsorption possible. Thus, the filler had a strong Cl^- adsorption ability and COD_{Cr} degradation ability. As can be seen, surface of the cavity wall inside the adsorbed filler ((C) and (D) of Fig. 8) was almost completely covered and attached to many folded crystals. Obviously, these crystalline substances were NaCl particles. The six-side body structure did not exist here because NaCl grew on a non-directional pattern on the irregular surface. Micro current was generated between the cathode and the anode in the process of micro-electrolysis, and a miniature electric field formed in the cavity. Na^+ and Cl^- moving in opposite directions may also lead to the formation of the folded crystal [21,22].

3.3. Treatment of actual salinity wastewater

To test the removal abilities of the iron-carbon alloy and the optimum reaction conditions, we studied three kinds of practical salinity wastewater through single-factor experiments. The effluent water quality was analyzed after the reaction. The COD_{Cr} removal rate of these practical wastewater samples was higher than 55%. The Cl^- removal rates were 27, 30 and 25%, respectively, (Fig. 8). Compared with the raw wastewater, these three kinds of wastewater after micro electrolysis process all had a remarkable increase in the oxygen consumption rate and a remarkable improvement in biodegradation. From Figs. 9–11, the oxygen consumption curves of wastewater after micro-electrolysis were high, indicating that the biodegradability of these three kinds of wastewater was improved significantly [23].

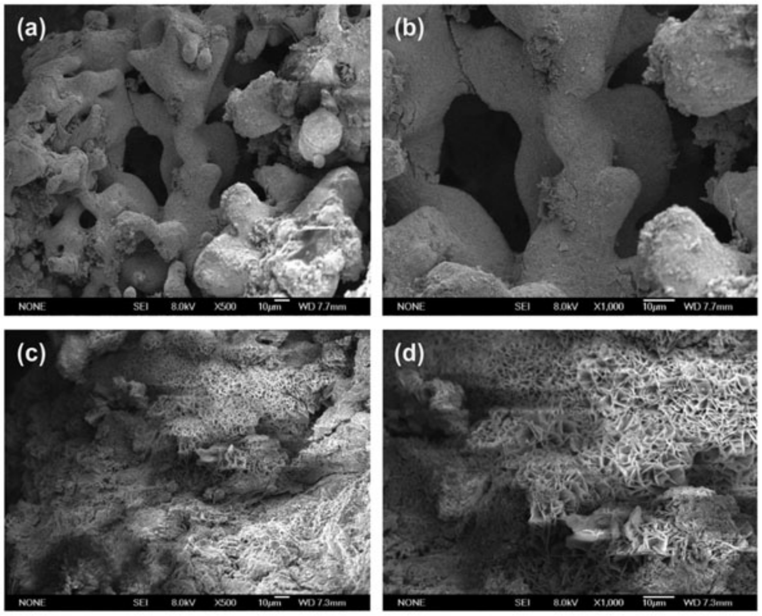

Fig. 7. SEM photograph of fillers before and after reaction.

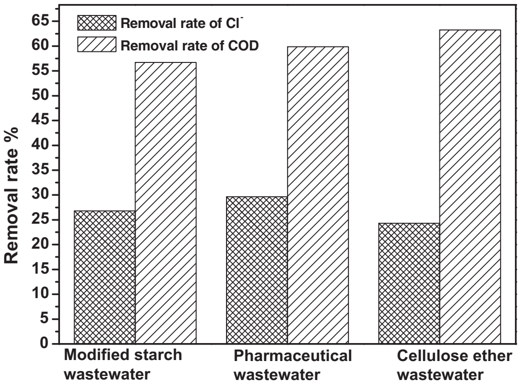

Fig. 8. Treatment effect of three kinds of high chloride wastewater.

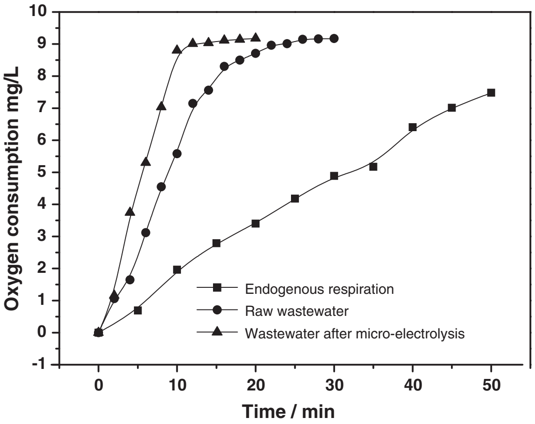

Fig. 9. Oxygen consumption curve of modified starch wastewater.

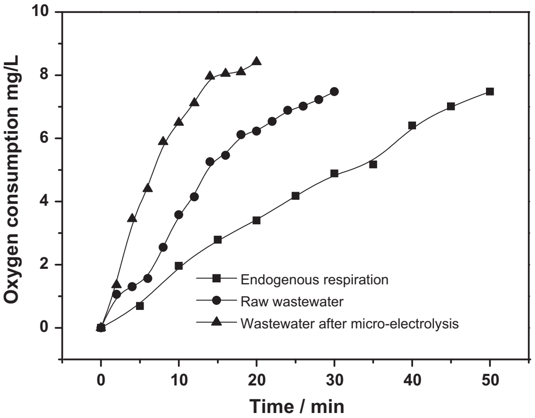

Fig. 10. Oxygen consumption curve of pharmaceutical wastewater.

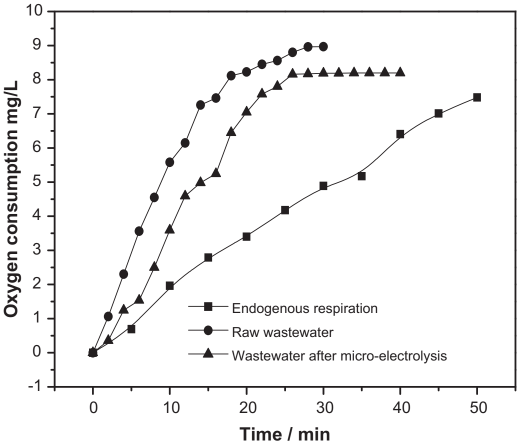

Fig. 11. Oxygen consumption curve of cellulose ether wastewater.

4. Conclusions

The iron-carbon alloy filler in this study had good treatment effect for Cl^- in wastewater. While there were many removal pathways including oxidizing Cl^- into Cl_2, flocculation, adsorption, etc., the main pathway was electric adsorption caused by micro-electrolysis process. XRD results showed that the filler had the capacity to adsorp NaCl. A SEM photograph revealed that there wasere a lot of cavities in the interior of the filler, making the formation of micro-electric field easy. The irregular cavity surface also caused the appearance of folded NaCl crystals.

For high salinity wastewater, micro-electrolysis with iron-carbon alloy was a feasible technology. Under optimum conditions, the COD_{Cr} removal rate of some wastewater was higher than 60% and the biodegradability of wastewater was greatly improved. The content of Cl^- had no inhibitory effect on the COD_{Cr} removal efficiency. This method was suitable for pretreatment of the salinity wastewater because of the simple process flow and shorter processing time.

Acknowledgements

This work was supported by the National Science and Technology Department Support Program (Typical Scrap Metal Products Recycling Technology and Application Research) under Grant No. 2011BAC10B04.

References

[1] M.A. Shannon, P.W. Bohn, M. Elimelech, J.G. Georgiadis, B.J. Marinas, A.M. Mayes, Science and technology for water purification in the coming decades, Nature 452 (2008) 301–310.

[2] P. Sherub, K.S. Ho, M. Tahir, E.S. Ibrahim, V. Saravanamuthu, K. Jaya, H. Seungkwan, L. Sangyoup, Blended fertilizers as draw solutions for fertilizer-drawn forward osmosis desalination, Environ. Sci. Technol. 46 (2012) 4567–4575.

[3] S. Liang, C. Liu, L.F. Song, Two-step optimization of pressure and recovery of reverse osmosis desalination process, Environ. Sci. Technol. 43 (2009) 3272–3277.

[4] Q.G. Jiang, Z.M. Ao, D.W. Chu, Q. Jiang, Reversible transition of graphene from hydrophobic to hydrophilic in the presence of an electric field, J. Phys. Chem. C 116 (2012) 19321–19326.

[5] L.H. Huang, G.P. Sun, T. Yang, B. Zhang, Y. He, X.H. Wang, A preliminary study of anaerobic treatment coupled with micro-electrolysis for anthraquinone dye wastewater, Desalination 309 (2013) 91–96.

[6] F. Ju, Y.Y. Hu, J.H. Cheng, Removal of chelated Cu(II) from aqueous solution by adsorption–coprecipitation with iron hydroxides prepared from microelectrolysis process, Desalination 274 (2011) 130–135.

[7] A. Sakalis, K. Mpoulmpasakos, U. Nickel, K. Fytianos, V. Voulgaropoulos, Evaluation of novel electrochemical pilot plant process for azo dyes removal from textile wastewater, Chem. Eng. J. 111 (2005) 63–70.

[8] M. Jeane, F. De, M. Rogerio, Iron and its sensitive balance in the cell, Mutation Res. 475 (2001) 153–159.

[9] H. Cheng, W. Xu, J. Liu, H. Wang, Y. He, G. Chen, Pretreatment of wastewater from triazine manufacturing by coagulation, electrolysis, and internal microelectrolysis, J. Hazard. Mater. 146 (2007) 385–392.

[10] Y.Z. Jin, Y.F. Zhang, W. Li, Micro-electrolysis technology for industrial wastewater treatment, J. Environ. Sci. 15 (2003) 334–338.

[11] Y. Wang, L. Wang, P. Peng, T. Lu, Treatment of naphthalene derivatives with iron-carbon micro-electrolysis, Trans. Nonferrous Met. Soc. China 16 (2006) 1442–1447.

[12] K. Rabaey, S. Butzer, S. Brown, J. Keller, R.A. Rozendal, High current generation coupled to caustic production using a lamellar bioelectrochemical system, Environ. Sci. Technol. 44 (2010) 4315–4321.

[13] X. Cao, X. Huang, P. Liang, K. Xiao, Y. Zhou, X. Zhang, B.E. Logan, A new method for water desalination using microbial desalination cells, Environ. Sci. Technol. 43 (2009) 7148–7152.

[14] State Environmental Protection Administration, Methods for the Examination of Water and Wastewater Analysis, China Environmental Science Press, Beijing, 2002.

[15] X. Yang, Interior microelectrolysis oxidation of polyester wastewater and its treatment technology, J. Hazard. Mater. 169 (2009) 480–485.

[16] J.C. Farmer, D.V. Fix, G.V. Mack, Capacitive deionization of NaCl and $NaNO_3$ solution with carbon aerogel electrodes, Electrochem. Soc. 143 (1996) 159–169.

[17] M. Maha, D.K. Patrick, F.C. Douglas, E.L. Bruce, Microbial electrodialysis cell for simultaneous water desalination and hydrogen gas production, Environ. Sci. Technol. 44 (2010) 9578–9583.

[18] X. Zhou, T. Korenaga, T. Takahashi, T. Moriwake, S. Shinoda, A process monitoring/controlling system for the treatment of wastewater containing chromium(VI), Water Res. 27 (1993) 1049–1054.

[19] Y.S. Evgenyi, F. Felix, Crystalline and amorphous phases in the ternary system water-sucrose-sodium chloride, J. Phys. Chem. 100 (1996) 1144–1152.

[20] P. Gianfranco, I. Francesc, N. Stelios, G.V. Constantinos, Quantum-chemical study of electrochemical promotion in catalysis, J. Phys. Chem. 100 (1996) 16653–16661.

[21] H.B. Li, L.D. Zou, L.K. Pan, Z. Sun, Novel graphene-like electrodes for capacitive deionization, Environ. Sci. Technol. 44 (2010) 8692–8697.

[22] Z.H. Huang, M. Wang, L. Wang, F. Kang, Relation between the charge efficiency of activated carbon fiberand its desalination performance, Langmuir 28 (2012) 5079–5084.

[23] S. Benjamin, E.D. Joanne, P.K. Judith, Kinetic analysis of oxygen utilization during cofactor biogenesis in a copper-containing amine oxidase from yeast, Biochemistry 39 (2000) 3699–3707.